beverages

MDPI

Article

Novel Method for the Identification of the Variety of Grape Using Their Capability to Form Gold Nanoparticles

Silvia Rodriguez [1], Beatriz de Lamo [1], Celia García-Hernández [1], Cristina García-Cabezón [2] and Maria Luz Rodríguez-Méndez [1,*]

[1] GroupUVaSens Department Inorganic Chemistry, Engineers School, Universidad de Valladolid, 47011 Valladolid, Spain; srodriguez_ross@hotmail.com (S.R.); beatriz.de.lamo.santamaria@gmail.com (B.d.L.); Celiagarciahernandez@gmail.com (C.G.-H.)

[2] Materials Science Group, Engineers School, Universidad de Valladolid, 47011 Valladolid, Spain; anacrigar@gmail.com

* Correspondence: mluz@eii.uva.es; Tel.: +34-983-423-540; Fax: +34-983-423-310

Received: 30 December 2017; Accepted: 19 March 2018; Published: 23 March 2018

Abstract: Gold nanoparticles (AuNPs) have been obtained using musts (freshly prepared grape juices where solid peels and seeds have been removed) as the reducing and capping agent. Transmission Electron Microscope images show that the formed AuNPs are spherical and their size increases with the amount of must used. The size of the AuNPs increases with the Total Polyphenol Index (TPI) of the variety of grape. The kinetics of the reaction monitored using UV-Vis shows that the reaction rates are related to the chemical composition of the musts and specifically to the phenols that can act as reducing and capping agents during the synthesis process. Since the particular composition of each must produces AuNPs of different sizes and at different rates, color changes can be used to discriminate the variety of grape. This new technology can be used to avoid fraud.

Keywords: gold nanoparticles; must; grapes

1. Introduction

The synthesis of gold nanoparticles is an active area of research, and a variety of techniques are currently available [1]. One of the most popular methods is the reduction of gold salts with an appropriate reducing agent, usually citrate. In recent years, green synthesis of gold nanoparticles (AuNPs) is gaining interest. In green synthesis, biomolecules (chitosan, polysaccharides, proteins, phenols, etc.) [2–7] and plant extracts (such as alfalfa, oats, coffee, onion, pear, banana, lemon grass extract, etc.) [8–11] are used as both the reducing agent and the stabilizer. AuNPs exhibit excellent physical, chemical and biological properties which are directly related to their size, shape and surface structure. For instance, AuNPs show a strong surface plasmon resonance (SPR) band in the visible region at ~520 nm [12,13] that is absent in bulk gold. The formation of gold nanoparticles can be detected by observing the color change of the solution. Moreover, the position, intensity and band-width of the SPR peaks rely on the nanoparticle size and shape [14,15]. Anions absorbed on the surface of nanoparticles stabilize the AuNPs avoiding aggregation. Different anions can be used to modulate the size and the color of the AuNPs. Size and shape dependent electrochemical and optical properties can be used for a wide range of applications, including chemical sensors for the assessment of the antioxidant capacity of foods [16–22]. According to these previous experiments, the optical properties of gold nanoparticles could be used to develop novel tools for the characterization of foods based on their antioxidant characteristics. Musts are extremely complex mixtures formed by

more than 300 components including among many others ions, sugars, organic acids and a variety of antioxidants. Phenols are one of the most important classes of antioxidants. The synthesis of gold nanoparticles with phytochemicals (mainly phenols) present in grape seeds and peels has been described [23]. Since different varieties of grapes contain different concentrations of polyphenols and capping agents, one could expect that the type of grape strongly affects the shape and size of the NPs. On this basis, the shape or size on AuNPs could be used by official agencies to detect frauds relative to the use of grapes of a different variety than the stated in the label.

The objective of this work was to evaluate the possibility of discriminating musts produced from grapes of different varieties by means of their capability to obtain AuNPs and to analyze the effect of the grape variety in the size and shape of the nanoparticles. For this purpose, musts obtained from eight different varieties of grapes—Cabernet Sauvignon (C), Garnacha (G), Juan García (JG), Mencía Regadio (MR), Mencía Secano (MS), Prieto Picudo (PP), Rufete (R), Tempranillo (T)—were used as reducing and capping agents. The effect of the total polyphenolic content was discussed.

2. Materials and Methods

Chloroauric acid ($HAuCl_4 \cdot 3H_2O$) was purchased from Sigma-Aldrich (St. Louis, MO, USA) and was used as received without any further purification. The deionized water used in preparation was obtained from Millipore Direct Q TM (resistivity of 18.2 MΩ). Red grapes of eight different Spanish varieties were used to obtain musts. The varieties included in the study were: Cabernet Sauvignon (C), Garnacha (G), Juan García (JG), Mencía Regadío (MR), Mencía Secano (MS), Prieto Picudo (PP), Rufete (R) and Tempranillo (T). They were provided by the oenological station Castilla Leon and several wineries. Musts were prepared following a method developed by the Instituto Tecnologico y Agrario de Castilla y León (ITACyl) (Valladolid, Spain). 100 berries of the given variety of grape were introduced in a plastic bag and crushed for 1 min. Then, peels and seeds were separated by centrifugation (10 min at 5000 rpm). Total Polyphenol Index (TPI) was measured using international standard methods by measuring the Absorbance at 280 nm [24]. These results are collected in Table 1 along with other parameters of interest.

Table 1. TPIs measured by chemical methods.

Variety of Grape	TPI	pH
Cabernet Sauvignon	14	3.17
Garnacha	17	3.17
Juan García	24	3.39
Mencía Regadío	19	3.96
Mencía Secano	19	3.93
Prieto Picudo	26	3.35
Rufete	27	3.37
Tempranillo	24	3.30

AuNPs were obtained using musts as the reducing and the capping agent by mixing a certain volume of the corresponding must with a certain volume of the chloroauric 0.01 M. The proportions used are shown in Table 2. In this manner, 9 samples of each grape variety were prepared by varying the gold/must between 9:1 and 1:9, while keeping all other concentrations constant. All experiments were carried out at ambient temperature and atmospheric pressure.

Table 2. Volumes of Au^{3+} and musts employed for the synthesis of AuNPs (mL). Dilutions are denoted as M1 to M9.

ID	M1	M2	M3	M4	M5	M6	M7	M8	M9
Au^{3+}	9	8	7	6	5	4	3	2	1
Must	1	2	3	4	5	6	7	8	9

UV-Vis Spectra of AuNPs by bio-reduction of chloroauric acid in aqueous solution was recorded in a Shimadzu spectrophotometer (mod UV 2603) (Kyoto, Japan) operated at a resolution of 1 nm in absorption mode. UV-Vis spectra were acquired between 400 and 700 nm. Water was used as the reference and the blank for baseline subtraction. The bioreduction (formation of nanoparticles) of $HAuCl_4$ in the aqueous solution was monitored following the plasmon resonance absorption band of the reaction mixture for 5 h.

In order to investigate the effect of the gold to must ratio on the particle size, Transmission Electron Microscope (TEM) images were recorded on a high-resolution electron microscope (HRTEM: JEOL JEM 2200) (Tokyo, Japan) operating at an accelerating voltage of 200 kV. Sample images were processed using Image J image processing software (public software). The samples were prepared by drop casting the AuNPs solution on a carbon-coated copper TEM grid. Principal Component Analysis (PCA) was carried out using the software Matlab v5.3. (The Mathworks Inc., Natick, MA, USA).

3. Results

Colloidal AuNPs were obtained at room temperature by reducing Au^{3+} using musts obtained from red grapes obtained from eight different varieties of grapes as the reducing agent. The ability of musts to form nanoparticles was evaluated by monitoring the color changes of the solutions. In order to optimize the synthesis, musts were mixed with the gold salt in different proportions as indicated in Table 2.

As a first step, the formation of nanoparticles was followed visually. As observed in Figure 1, the color of the suspension changed upon addition of the gold salt from pale pink to dark purple which indicated the formation of AuNPs. The reaction started immediately and continued for several hours. It is worth noting that the extent of the reaction was dependent on the Au^{3+}:must ratio used, and also on the variety of grape; that is, on the chemical composition of the must (reduction capability and capping agents).

Figure 1. Response of mixtures of Au^{3+} salt and musts obtained from (**a**) Cabernet; (**b**) Garnacha; (**c**) Juan García; (**d**) Mencía Secano; (**e**) Mencía Regadío; (**f**) Prieto Picudo; (**g**) Rufete and (**h**) Tempranillo grapes. **Left column** corresponds to photographs taken 5 min after the mixture. **Right column** corresponds to photographs taken 3 h after the mixture. Ten tubes inside each picture correspond to increasing Au^{3+}:must ratios as indicated in Table 1.

The formation of AuNPs was monitored using UV-Vis spectroscopy (Figure 2). All spectra showed a broad absorption peak between 500 and 600 nm corresponding to the SPR band consistent with Mie theory [25,26], which establishes that the position of the SPR band is related to the size of AuNPs. In this case, the intensities and positions of the SPR bands were dependent on the nature of the grape used to obtain the musts. Since musts prepared from different varieties of grape have different compositions, the variety of colors obtained suggested that AuNPs could be used to analyze grapes.

For the smallest must volume (M1 where Au^{3+}:must = 9:1) the observed plasmon band was weak and appeared at ca. 580 nm. As the Au^{3+}:must ratio increased, a notable rise in the intensity of the SPR band was observed, confirming the increase in the number of nanoparticles obtained. Simultaneously, the position of the band shifted to lower wavelengths (at ca. 520 nm), suggesting growth of the nanoparticle size when increasing the reagent ratio. This is in good correlation with previous studies that have demonstrated that the size of the obtained nanoparticles depends on the concentration of the reducing agent (citrate, nitrite, etc.), and that this effect can be used to develop colorimetric probes [27,28]. A further observation from analysis of these spectra concerns the broadness of the peaks that are reflecting of a large dispersion of the size of the AuNPs obtained.

Similar trends were observed in most of the varieties analyzed. However, the spectral changes were smaller in those varieties of grapes with lower TPI in the whole range of 5 min–5 h. Figure 2 illustrates how the intensity of the peaks increase linearly with concentration.

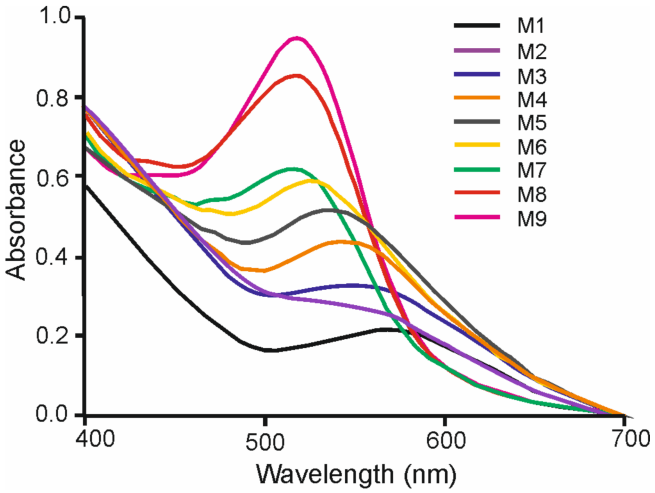

Figure 2. UV-Vis spectra of Au^{3+}:must Cabernet mixtures in proportions M1 to M9.

TEM images provided information about the morphology of the obtained AuNPs that confirms the information obtained from the UV-Vis absorption spectra. Figure 3 shows the images of the AuNPs obtained from Tempranillo must using different ratios Au^{3+}:must. The nanoparticles obtained showed a reasonable uniform size. When increasing the ratio Au^{3+}:must from M1 to M9, the size of the AuNPs increased from 5 to 60 nm.

In addition, the size and shape of the obtained nanoparticles changed with the type of must.

A closer look to the AuNPs revealed interesting features. In the case of Tempranillo grapes, the nanoparticles obtained were nearly spherical in shape, but, gold nanostructures with branched arms were also observed. This dual structure containing spherical nanoparticles and branched structures could indicate that two different growth mechanisms were involved. When increasing the Au^{3+}:must ratio from M1 to M9, the size of the AuNPs increased and the size of the branched arms grows simultaneously (Figure 4). The size and shape of the obtained nanoparticles changed with the type of must. When musts with low TPI were used as reducing agent, a larger number of AuNPs was obtained, and the shapes were not spherical. Instead, they were triangular or hexagonal. This is illustrated in Figure 5 for the AuNPs obtained using Garnacha grapes in ratio M1.

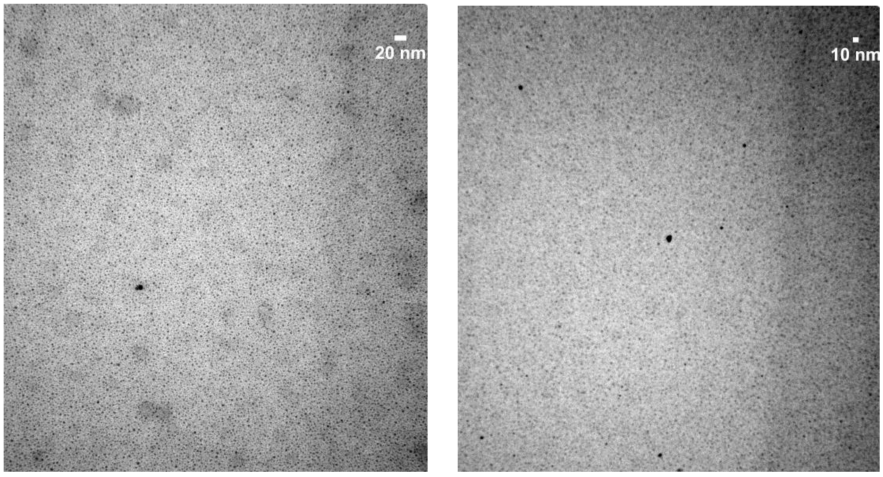

Figure 3. TEM images of the AuNPs obtained using Tempranillo must using (**a**) ratio M5; (**b**) ratio M9. Pictures taken at 2,000,000×; 80 K.

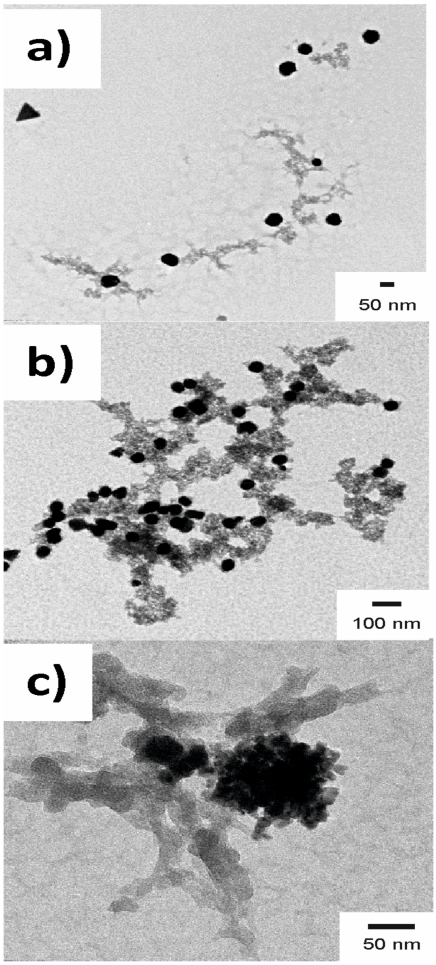

Figure 4. TEM images of the AuNps obtained using Tempranillo must using (**a**) M1; (**b**) M5 and (**c**) M9 ratios.

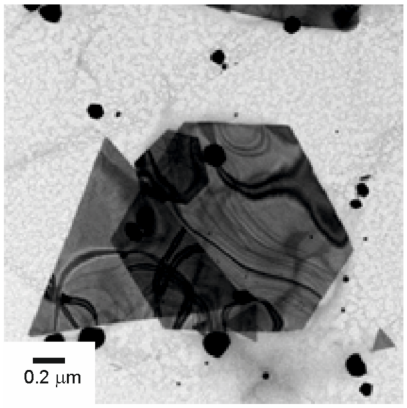

Figure 5. TEM images of the AuNps obtained using Garnacha must using Au^{3+}:must ratio 9:1.

As shown in the previous paragraphs, musts obtained from different varieties of grapes produced different amounts of AuNPs. Changes in color also indicate that some varieties of grape produce faster reactions than others. The kinetics of the reactions was studied using UV-Vis spectroscopy using three Au^{3+}:must ratios (M1, M5 and M9) for the different types of grapes. UV-Vis spectra were registered periodically after the addition of the corresponding must. Results are shown in Figure 6.

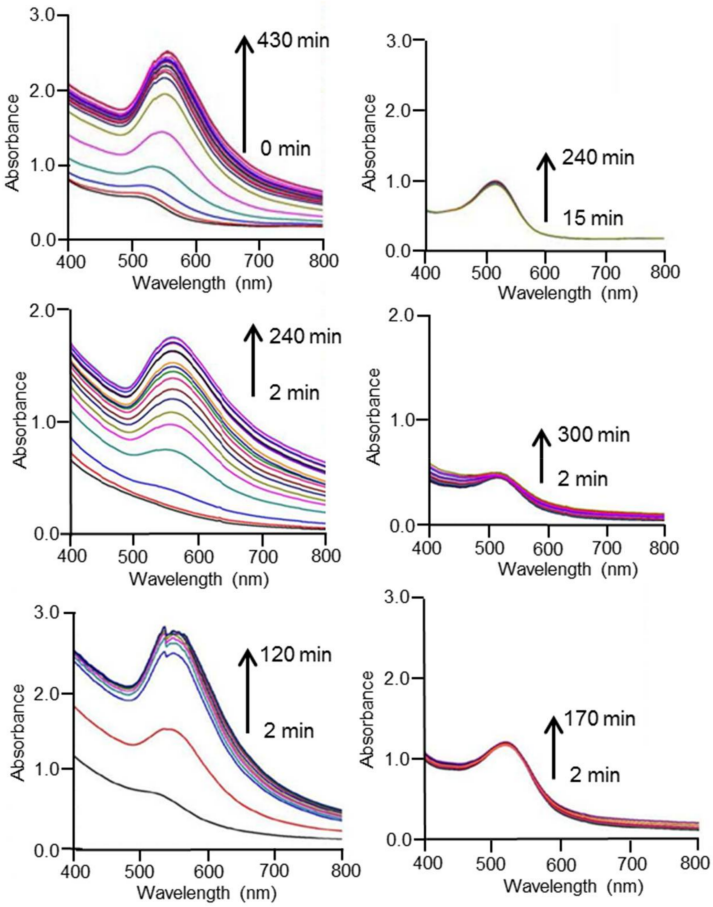

Figure 6. UV-Vis spectra of Au^{3+}:must mixtures in M1 (**left**) and M9 (**right**) using a must with low TPI (upper specta: Cabernet-Sauvignon), a must with medium TPI (middle spectra: Mecía Secano) and a must with high TPI (lower spectra: Tempranillo).

In all grapes studied, the absorbance increased progressively with time, confirming the formation of AuNPs. Then, a plateau was attained. The time elapsed before the constant value was reached was ca. 300 min when using varieties with low TPI such as Cabernet-Sauvignon. The time necessary to attain the plateau was ca. 180 min for varieties, such as Mancía Secano, with intermetadiate TPI values, and 50 min when varieties, such as Tempranillo, with high TPI were used. This result confirmed the influence of the antioxidant capacity in the AuNP formation.

Figure 7 illustrates the variation of the absorbance and the wavelength of the plasmon peak with time for the variety Tempranillo. Then, a plateau was reached. When AuNPs are formed using the proportion M1, the concentration of reducing compounds was small, and the formation rate of AuNPs was slow, as indicated by the slow changes in absorbance and wavelength observed. The rate of AuNP formation was faster using the proportion M5, where the formation of AuNPs was completed in a few seconds. In the case of the proportion M9, the formation rate was so fast that at the first measurement, the AuNPs had already been formed. The kinetics of the reaction analyzed by representing the slope of the change of absorbance with time (measured from 2 min after the addition until stabilization of the signal) confirmed the influence of the concentration of reactants in the formation rate. The rest of the musts showed similar trends, and reaction rates were directly related to the TPI values. Since the particular composition of each must produce AuNPs with different sizes and at different rates, color changes can be used to discriminate the variety of grape.

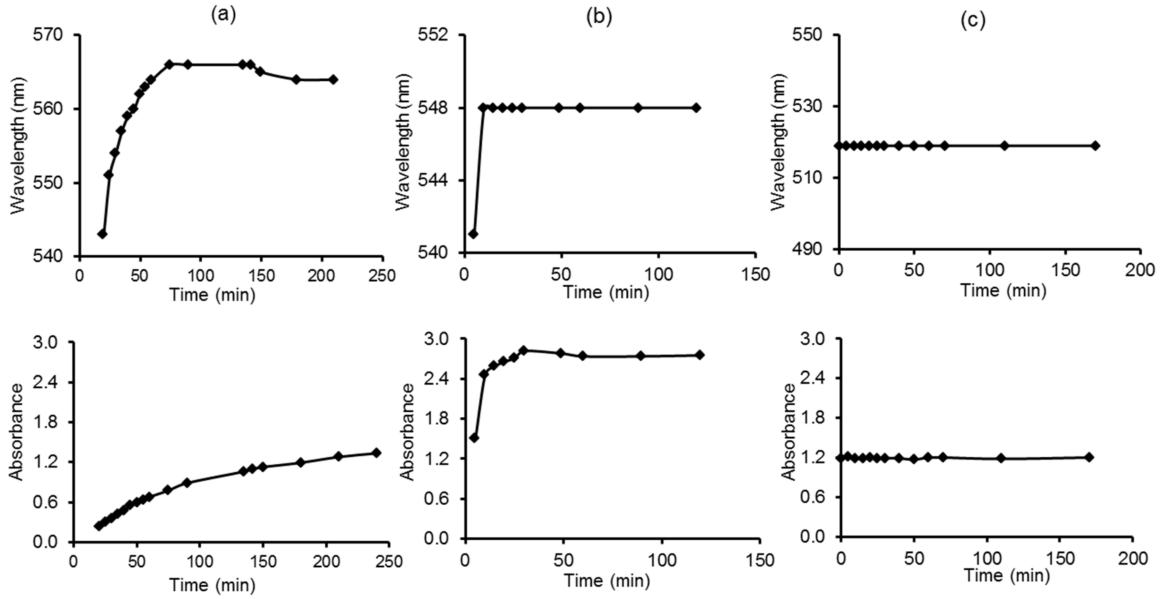

Figure 7. Variation of the wavelength and the absorbance with time during AuNPs formation using Tempranillo must (**a**) M1; (**b**) M5 (**c**) M9.

4. Discussion and Conclusions

Must-stabilized AuNPs of different diameters were prepared using grape juice. The influence of the proportion of grape juice and the variety of grape was analyzed. UV-Vis and TEM images show that when increasing the concentration of reactants, the particle size and the reaction rate increased simultaneously. Because musts prepared from different varieties of grape possess distinct chemical compositions, AuNPs of different sizes are obtained from different grapes. The particular reactivity shown by different variety of grapes produce AuNPs with different colors and with distinct kinetics. These observations can be used to discriminate grapes of different varieties and to analyze their phenolic content.

Acknowledgments: Financial support by MINECO and FEDER (AGL2015-67482-R) and the Junta de Castilla y León (VA011U16) is gratefully acknowledged. C.G.-H thanks for the grant of JCYL (BOCYL-D-24112015-9). S.R. would like to acknowledge EMA2 EURICA program for the scholarship granted.

Author Contributions: S.R., B.d.L. and C.G.-H. carried out the experiments. C.G.-C. interpreted the results. M.L.R.-M. interpreted the results, obtained the funds and wrote the paper.

Conflicts of Interest: Authors declare no conflicts of interest or state. The founding sponsors had no role in the design of the study; in the collection, analyses, or interpretation of data; in the writing of the manuscript, and in the decision to publish the results.

References

1. Zhao, P.; Li, N.; Astruc, D. State of the art in gold nanoparticle synthesis. *Coord. Chem. Rev.* **2013**, *257*, 638–665. [CrossRef]
2. Anuradha, S.; Anand, V.R.; Hemanth, K. Surface modification of chitosan for selective surface–protein interaction. *Carbohydr. Polym.* **2006**, *66*, 321–332. [CrossRef]
3. Bhumkar, D.R.; Joshi, H.M.; Sastry, M.; Pokharkar, A.V. Chitosan Reduced Gold Nanoparticles as Novel Carriers for Transmucosal Delivery of Insulin. *Pharmacol. Res.* **2007**, *24*, 1415–1426. [CrossRef] [PubMed]
4. Malathi, S.; Balakumaran, M.D.; Kalaichelvan, P.T.; Balasubramanian, S. Green synthesis of gold nanoparticles for controlled delivery. *Adv. Mater. Lett.* **2013**, *4*, 933–940. [CrossRef]
5. Schulz, A.; Wang, H.; Van Rijin, P.; Boker, A. Synthetic inorganic materials by mimicking biomineralization processes using native and non-native protein functions. *J. Mater. Chem.* **2011**, *21*, 18903. [CrossRef]
6. Arakaki, A.; Shimizu, K.; Oda, M.; Sakamoto, T.; Nishimura, T.; Kato, T. Biomineralization-inspired synthesis of functional organic/inorganic hybrid materials: Organic molecular control of self-organization of hybrids. *Org. Biomol. Chem.* **2015**, *13*, 974–989. [CrossRef] [PubMed]
7. Galloway, J.M.; Staniland, S.S. Protein and peptide biotemplated metal and metal oxide nanoparticles and their patterning onto surfaces. *J. Mater. Chem.* **2012**, *22*, 12423–12434. [CrossRef]
8. Gardea-Torresdey, J.L.; Parsons, J.G.; Gomez, E.; Peralta-Videa, J.; Troiani, H.E.; Santiago, P.; Jose-Yacaman, M. Formation and Growth of Au Nanoparticles inside Live Alfalfa Plants. *Nano Lett.* **2002**, *2*, 397–401. [CrossRef]
9. Bankar, A. Banana peel extract mediated synthesis of gold nanoparticles. *Coll. Surf. B Biointerfaces* **2010**, *80*, 45–50. [CrossRef] [PubMed]
10. Huang, J.; Li, Q.; Sun, D.; Lu, Y.; Su, Y.; Yang, X.; Wang, H.; Wang, Y.; Shao, W.; He, N.; et al. Biosynthesis of Silver and Gold Nanoparticles by Novel Sundried Cinnamon camphora Leaf. *Nanotechnology* **2007**, *18*, 105104. [CrossRef]
11. Shankar, S.S.; Rai, A.; Ankamwar, B.; Singh, A.; Ahmad, A.; Sastry, M. Biological Synthesis of Triangular Gold Nanoprisms. *Nat. Mater.* **2004**, *3*, 482–488. [CrossRef] [PubMed]
12. Haiss, W.; Thanh, N.T.; Aveyard, J.; Fernig, A.D. Determination of Size and Concentration of Gold Nanoparticles from UV-Vis Spectra. *Anal. Chem.* **2007**, *79*, 4215–4221. [CrossRef] [PubMed]
13. Sharma, A.; Singh, B.P.; Gathania, A.K. Synthesis and characterization of dodecanothiol-stabilized gold nanoparticles. *Indian J. Pure Appl. Phys.* **2014**, *52*, 93–100.
14. Olson, J.; Dominguez-Medina, S.; Hoggard, A.; Wang, L.; Chang, W.W.; Link, S. Optical Characterization of Single Plasmonic Nanoparticles. *Chem. Soc. Rev.* **2015**, *44*, 40–57. [CrossRef] [PubMed]
15. Yang, X.; Yang, M.; Pang, B.; Vara, M.; Xia, Y. Gold nanomaterials at work in biomedicine. *Chem. Rev.* **2015**, *115*, 10410–10488. [CrossRef] [PubMed]
16. Cobley, C.M.; Chen, J.; Cho, E.C.; Wang, L.V.; Xia, Y. Gold nanostructures: A class of multifunctional materials for biomedical applications. *Chem. Soc. Rev.* **2011**, *40*, 44–56. [CrossRef] [PubMed]
17. Kong, D.; Liu, L.; Song, S.; Suryoprabowo, S.; Li, A.; Kuang, H.; Wang, L.; Xu, Ch. A gold nanoparticle-based semi-quantitative and quantitative ultrasensitive paper sensor for the detection of twenty mycotoxins. *Nanoscale* **2016**, *8*, 5245–5253. [CrossRef] [PubMed]
18. Medina-Plaza, C.; García-Cabezón, C.; García-Hernández, C.; Bramorski, C.; Blanco-Val, Y.; Martín-Pedrosa, F.; Kawai, T.; de Saja, J.A.; Rodríguez-Méndez, M.L. Analysis of organic acids and phenols of interest in the wine industry using Langmuir-Blodgett films based on functionalized nanoparticles. *Anal. Chim. Acta* **2015**, *853*, 572–578. [CrossRef] [PubMed]

19. Medina-Plaza, C.; Furini, L.N.; Constantino, C.J.L.; de Saja, J.A.; Rodríguez-Mendez, M.L. Synergistic electrocatalytic effect of nanostructured mixed films formed by functionalised gold nanoparticles and bisphthalocyanines. *Anal. Chim. Acta* **2014**, *851*, 95–102. [CrossRef] [PubMed]
20. Yola, M.L.; Atar, N.A. Novel voltammetric sensor based on gold nanoparticles involved in p-aminothiophenol functionalized multi-walled carbon nanotubes: Application to the simultaneous determination of quercetin and rutin. *Electrochim. Acta* **2014**, *119*, 24–31. [CrossRef]
21. Vilela, D.; González, M.C.; Escarpa, A. Nanoparticles as analytical tools for in-vitro antioxidant-capacity assessment and beyond. *Trends Anal. Chem.* **2015**, *64*, 1–16. [CrossRef]
22. Vilela, D.; González, M.C.; Escarpa, A. Gold-nanosphere formation using food sample endogenous polyphenols for in-vitro assessment of antioxidant capacity. *Anal. Bioanal. Chem.* **2012**, *404*, 341–349. [CrossRef] [PubMed]
23. Amarnath, K.; Mathew, N.L.; Nellore, J.; Siddarth, C.R.V.; Kumar, J. Facile synthesis of biocompatible gold nanoparticles from Vitis vinifera and its cellular internalization against HBL-100 cells. *Cancer Nanotechnol.* **2011**, *2*, 121–132. [CrossRef] [PubMed]
24. International Organisation of Vine and Wine (OIV). Compendium of International Methods of Analysis of Wines and Musts. In *Bulletin de L'organisation Internationale de la Vigne et du Vin*; OIV: Paris, France, 2013.
25. Klar, T.; Perner, M.; Grosse, S.; Von Plessen, G.; Spirkl, W.; Feldmann, J. Surface-Plasmon Resonances in Single Metallic Nanoparticles. *Phys. Rev. Lett.* **1998**, *80*, 4249–4252. [CrossRef]
26. Kelly, K.L.; Coronado, E.; Zhao, L.L.; Schatz, G.C. The optical properties of metal nanoparticles: The influence of size, shape, and dielectric environment. *J. Phys. Chem. B* **2003**, *107*, 668–677. [CrossRef]
27. Nama, Y.S.; Noh, K.C.; Kim, N.K.; Lee, Y.; Park, H.K.; Lee, K.B. Sensitive and selective determination of NO2 ion in aqueous samples using modified gold nanoparticle as a colorimetric probe. *Talanta* **2014**, *125*, 153–158. [CrossRef] [PubMed]
28. Medina-Plaza, C.; Rodriguez-Mendez, M.L.; Sutter, P.; Tong, X.; Sutter, E. Nanoscale Au-In alloy-oxide core-shell particles as electrocatalysts for efficient hydroquinone detection. *J. Phys. Chem. C* **2015**, *119*, 25100–25107. [CrossRef]